ORGANIC LETTERS

2008
Vol. 10, No. 6
1287−1290

Competing Isomerizations of [12]Annulenes: Diels–Alder Reaction versus Electrocyclization

Claire Castro,*,† William L. Karney,†,‡ Elizabeth Noey,† and K. Peter. C. Vollhardt*,§

Departments of Chemistry and Environmental Science, University of San Francisco, 2130 Fulton Street, San Francisco, California 94117-1080, and Department of Chemistry, University of California at Berkeley, Berkeley, California 94720-1460

castroc@usfca.edu; kpcv@berkeley.edu

Received January 26, 2008

ABSTRACT

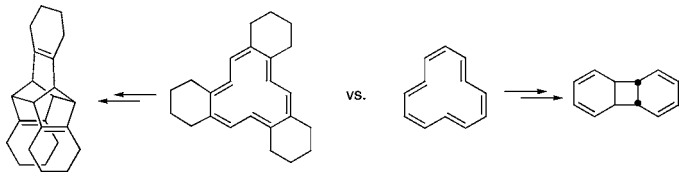

Experimentally, tri-*trans*-[12]annulene and tris(cyclohexeno)[12]annulene exhibit differing reactivities. Whereas the former, after isomerizing to its di-trans isomer, undergoes sequential electrocyclizations, the latter follows a Diels–Alder pathway after initial electrocyclization. B3PW91/6-31+G*//B3LYP/6-31G* calculations indicate that cyclohexenofusion simultaneously hinders the second electrocyclization and facilitates Diels–Alder reaction, primarily by inducing greater puckering in the intermediate eight-membered ring.

Understanding the chemistry of annulenes continues to interest researchers in organic chemistry.[1] This interest arises from a desire to understand aromaticity of both planar and nonplanar topologies,[2,3] coupled with the use of annulene derivatives to generate carbon-rich materials.[4] Substituents attached to annulenes can influence profoundly the core's properties and reactivity. For example, benzofused systems experience a pronounced decrease in aromaticity due to the Clar effect for [4*n*+2]-Hückel and [4*n*]-Möbius topologies.[5,6] Substituents also affect dynamic processes of the polyene nucleus. Vollhardt et al.[7] recently suggested that cyclohexenofused [12]annulene **2** was the product of sequential cyclobutene ring-opening of precursor **1** (Scheme 1). They

Scheme 1

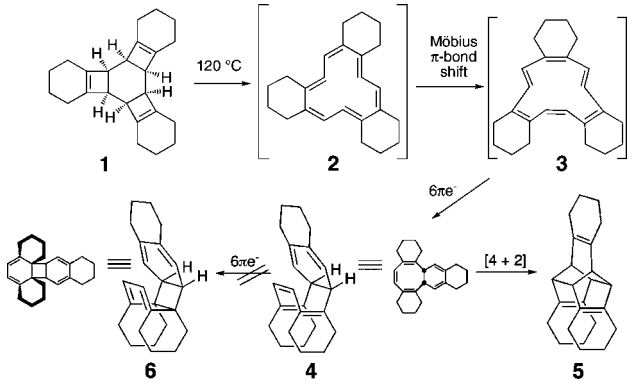

proposed that **2** undergoes thermal Möbius π-bond shift[8] to substituted di-trans isomer **3**, which then forms the observed cage compound **5** in two steps: thermal electrocyclization followed by [4+2]cycloaddition. In contrast, the benzofused

† Department of Chemistry, University of San Francisco.
‡ Department of Environmental Science, University of San Francisco.
§ University of California at Berkeley.

(1) Spitler, E. L.; Johnson, C. A.; Haley, M. M. *Chem. Rev.* **2006**, *106*, 5344.
(2) Schleyer, P. v. R., Ed. *Chem. Rev.* **2001**, *101*, May issue.
(3) Rzepa, H. S. *Chem. Rev.* **2005**, *105*, 3697.
(4) Haley, M. M.; Tykwinski, R. R., Eds. *Carbon-Rich Materials: From Molecules to Materials*; Wiley-VCH: Weinheim, 2006.
(5) Clar, E. *The Aromatic Sextet*; Wiley: London, 1972.
(6) For an example of a benzofused Möbius annulene and the discussion of its aromaticity see, (a) Ajami, D.; Oeckler, O.; Simon, A.; Herges, R. *Nature* **2003**, *426*, 819. (b) Castro, C.; Chen, Z.; Wannere, C. S.; Jiao, H.; Karney, W. L.; Mauksch, M.; Puchta, R.; Hommes, N. J. R. v. E.; Schleyer, P. v. R. *J. Am. Chem. Soc.* **2005**, *127*, 2425.
(7) Eichberg, M. J.; Houk, K. N.; Lehmann, J.; Leonard, P. W.; Märker, A.; Norton, J. E.; Sawicka, D.; Vollhardt, K. P. C.; Whitener, G. D.; Wolff, S. *Angew. Chem., Int. Ed.* **2007**, *46*, 6894.

10.1021/ol8001915 CCC: $40.75
Published on Web 02/27/2008

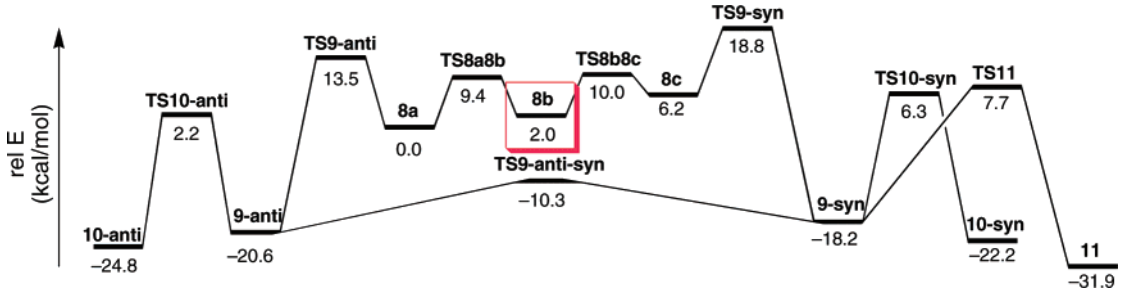

Figure 1. CCSD(T)/cc-pVDZ//B3LYP/6-31G* potential energy graph for the conversion of di-*trans*-[12]annulene **8b** to either benzene dimer **10** or cage compound **11**.

analog of **1** (in which the three peripheral cyclohexene rings are replaced by benzene) unraveled by concerted [$\sigma^2_s+\sigma^2_s+\sigma^2_s$] retrocyclization to the corresponding all-cis-tribenzo-[12]-annulene in which π-bond shift is energetically prohibited by loss of benzene ring aromaticity.

We were very interested in the reaction path of **2** outlined in Scheme 1, as it does not follow that put forth by Oth and Schröder for the parent tri-*trans*-[12]annulene **7** (Scheme 2).[9]

Scheme 2

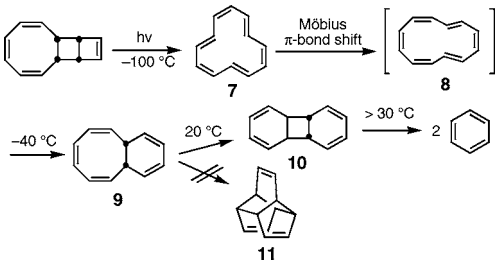

Whereas the first two steps are the same, namely Möbius π-bond shift to di-trans isomer **8**, followed by electrocyclization, Oth and Schröder observed benzene as the final product, not cage compound **11**. Benzene arises from **9** by a second 6π closure to give initially its dimer **10**, which dissociates readily.[10]

Why the divergence in reactivity after the first electrocyclization to construct the cis-bicyclic frame of **4** and **9**, respectively? What role does cyclohexenofusion play in controlling the reactivity? Given the interest in designing hydrocarbons with new topologies,[11] especially carbon-rich materials, understanding these fundamental issues should help in fine-tuning strategies for the synthesis of annulenes, as well as understanding their reactivity.

Because of the size of the substituted system, the original computational results for the reaction path leading to **5** (Scheme 1) were generated at the B3LYP/6-31G* level.[7] However, in a comparative computational investigation of hydrocarbon isomer energy differences, Schreiner and Fokin found that this method can lead to large errors—errors that increase with system size.[12] These shortcomings are most notable when comparing isomers that differ in the relative numbers of single and double bonds, exactly the scenario encountered in electrocyclizations. For systems that are too large for higher level CCSD(T) single point calculations, the Schreiner/Fokin team suggests using the B3PW91 functional for the determination of relative energies. We therefore recomputed the energies of species **3**–**6**, along with the transition states toward **5** and **6**, with this method (Table 1).[13,14]

Table 1. Relative Energies (kcal/mol) of Cyclohexenofused [12]Annulenes and Valence Isomers in Scheme 1

species	sym	NI	B3LYP/6-31G*[a,b]	B3PW91/6-31+G*[a,b]
3	C_1	0	0.0	0.0
4-syn	C_1	0	−9.8	−13.3
4-anti	C_1	0	−7.8	−11.5
5	C_2	0	−22.7	−33.1
6-syn	C_1	0	−11.2	−16.6
6-anti	C_1	0	−8.5	−14.3
TS5	C_1	1	12.8	5.8
TS6-syn	C_1	1	17.2	12.9
TS6-anti	C_1	1	16.9	12.6

[a] Values differ from those presented in ref 7 because the energies presented here are relative to a more stable di-trans conformation of **3**. In ref 7, energies were given relative to the conformation analogous to **8c** in Scheme 3. [b] Relative energies corrected for ZPE differences.

In contrast to the substituted system, [12]annulene is small enough to permit higher level calculations. Thus, we obtained both B3PW91/6-31+G*//B3LYP/6-31G* and CCSD(T)/cc-pVDZ//B3LYP/6-31G* single point energies for the $C_{12}H_{12}$ isomers involved in the reactions that lead to both stereoisomers of benzene dimer **10** and cage compound **11** (Table 2).[13,14] The pathway from di-*trans*-[12]annulene **8** to

(8) Moll, J. F.; Pemberton, R. P.; Gutierrez, M. G.; Castro, C.; Karney, W. L. *J. Am. Chem. Soc.* **2007**, *129*, 274, and references therein.
(9) Oth, J. F. M.; Röttele, G.; Schröder, G. *Tetrahedron Lett.* **1970**, 61.
(10) (a) Gan, H.; Horner, M. G.; Hrnjez, B. J.; McCormack, T. A.; King, J. L.; Gasyna, Z.; Chen, G.; Gleiter, R.; Yang, N.-c. C. *J. Am. Chem. Soc.* **2000**, *122*, 12098. (b) Noh, T.; Gan, H.; Halfon, S.; Hrnjez, B. J.; Yang, N.-c. C. *J. Am. Chem. Soc.* **1997**, *119*, 7470.
(11) Herges, R. *Chem. Rev.* **2006**, *106*, 4820.
(12) (a) Schreiner, P. R.; Fokin, A. A.; Pascal, R. A.; de Meijere, A. *Org. Lett.* **2006**, *8*, 3635. (b) Schreiner, P. R. *Angew. Chem., Int. Ed.* **2007**, *46*, 4217.

Table 2. Relative Energies (kcal/mol) of $C_{12}H_{12}$ Species Presented in Scheme 3 and Related Transition States

species	sym	B3LYP/6-31G* NI	B3LYP/6-31G* rel E^b	B3PW91/6-31+G*[a] rel E^b	CCSD(T)/cc-pVDZ[a] rel E^b
7	C_1	0	−3.9	−3.7	−4.0
8a	C_s	0	0.0	0.0	0.0
8b	C_1	0	2.6	2.4	2.0
8c	C_s	0	9.5	9.1	6.2
9-syn	C_1	0	−12.5	−16.4	−18.2
9-anti	C_1	0	−14.7	−18.8	−20.6
10-syn	C_2	0	−15.6	−22.0	−22.2
10-anti	C_2	0	−19.0	−25.6	−24.8
11	C_{2v}	0	−14.1	−26.1	−31.9
TS8a8b	C_1	1	10.7	10.3	9.4
TS8b8c	C_1	1	10.4	10.0	10.0
TS9-syn-anti	C_1	1	−7.2	−11.1	−10.3
TS9-anti	C_s	1	12.9	10.7	13.5
TS9-syn	C_s	1	19.5	17.3	18.8
TS10-anti	C_1	1	6.7	1.0	2.2
TS10-syn	C_1	1	10.6	5.3	6.3
TS11	C_s	1	18.9	10.4	7.7

[a] Relative energies computed at the B3LYP geometries. [b] Relative energies corrected for differences in ZPE.

10 and **11** is presented in Scheme 3. Figure 1 shows a CCSD(T) potential energy graph for the dynamic processes outlined in Scheme 3 (see Supporting Information for geometries of relevant stationary points).

Scheme 3

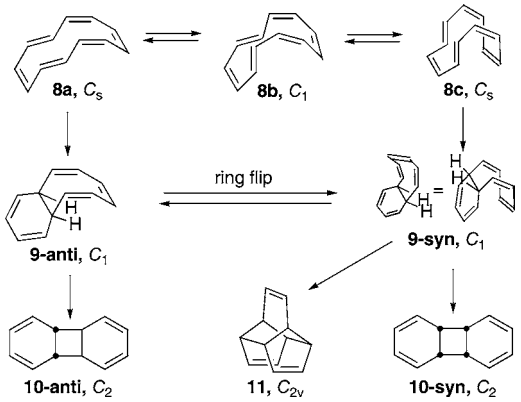

In the case of the cyclohexenofused system, the data in Table 1 support the experimental observation that the lowest energy path is that leading to Diels−Alder adduct **5**. Both DFT methods predict that **4-syn**, the conformation necessary for the cycloaddition reaction, is more stable than **4-anti** by ca. 2 kcal/mol. The barrier for the Diels−Alder process (19.1 kcal/mol, B3PW91/6-31+G*//B3LYP/6-31G*, from **4-syn**) is ca. 7 kcal/mol less than that for forming either substituted benzene dimer **6-syn** or **6-anti**. Finally, as anticipated, the B3PW91 relative energies are lower than those obtained from B3LYP, the most significant difference noted in the case of **5** (the greatest change in the number of double bonds).

Turning to the parent system, both DFT and coupled cluster methods reveal that the reaction path with the smallest overall barrier from di-*trans*-[12]annulene **8b** is that which affords benzene dimer **10-anti** (Table 2, Figure 1), in agreement with the experimental results. However, within the reaction scheme there is a shift in the energetic ordering of the stationary points between B3LYP and CCSD(T) (vide infra). The discussion below pertains to CCSD(T) results, unless otherwise noted.

The initial conformation of di-*trans*-[12]annulene that results from Möbius π-bond shifting in tri-*trans*-[12]-annulene is **8b**. It connects to two other conformations on the potential energy surface, the slightly more stable **8a** and the less stable **8c**. Whereas **8a** and **8c** can undergo thermal ring closure to **9-anti** and **9-syn**, respectively, assembly of the cage compound **11** requires **9-syn** (Scheme 3). The lowest energy path to **9-syn** is **8b** → **8a** → **9-anti** → **9-syn** (E_a = 11.5 kcal/mol). From **9-syn**, [4+2] cycloaddition provides **11** (E_a = 25.9 kcal/mol). Generation of dimer **10-syn** from **9-syn** is modestly more favorable (E_a = 24.5 kcal/mol) (Figure 1).

Although the above outlines a route to **10-syn** and **11**, an apparently even lower energy alternative for the parent di-*trans*-[12]annulene **8** is the trajectory that Oth and Schröder found−namely ring closure to the observed bicyclic **9-anti**, followed by a second cyclization to benzene dimer **10-anti** (Schemes 2 and 3, Figure 1), which then produces benzene in a highly exothermic step.[10]

Although B3LYP energies indeed predict that formation of **10-anti** would be favored, this method appears to grossly overestimate the energy cost toward cage compound **11** (via **TS11**). CCSD(T) lowers this barrier considerably, making this reaction nearly competitive with that en route to benzene dimer **10-syn**. Moreover, in contrast to B3LYP, CCSD(T) prefers cage compound **11** over dimer **10-anti**. This switch in energetic ordering when changing from B3LYP to CCSD(T) is consistent with the Schreiner/Fokin study. In additional agreement with their conclusions, B3PW91/6-31+G* single point calculations gave results much closer to those obtained with CCSD(T). This validation of the B3PW91 method is important, since, for the more highly substituted case, there is no complete set of CCSD(T) data available.

The differences in reactivity of the parent and substituted systems are exemplified by the branching points **4-syn** and **9-syn** (Figure 2). The addition of the fused rings influences the choice between the two possible final steps in two ways. First, it raises the barrier for the second electrocyclization step by 4−5 kcal/mol, and second, it lowers the barrier for

(13) Geometry optimizations and vibrational analyses were performed using B3LYP/6-31G*. This method is known to be adequate for obtaining geometries for use in subsequent single point calculations (see ref 12). B3PW91/6-31+G* and CCSD(T)/cc-pVDZ single point energies were computed using the B3LYP/6-31G* geometries.

(14) All calculations were performed using Gaussian 03. Frisch, M. J. et al.; *Gaussian 03*, revision C.02; Gaussian, Inc.: Wallingford, CT, 2004. See Supporting Information for full citation.

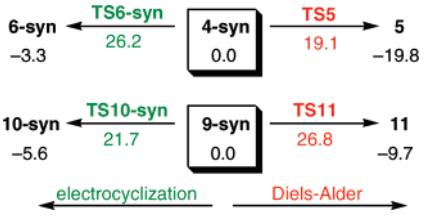

Figure 2. B3PW91/6-31+G*//B3LYP/6-31G* + ZPE energetics for electrocyclization vs Diels−Alder reaction in **4-syn** and **9-syn**. Relative energies are given in kcal/mol.

Diels−Alder reaction by 7−8 kcal/mol. To understand the reason for this shift in reactivity, we determined the barriers for electrocyclization in cyclooctatriene model systems (**12**−**14**).

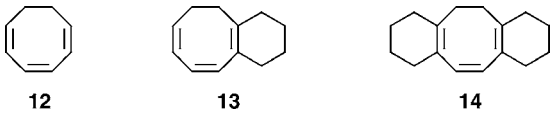

They increase from 23.7 kcal/mol for **12**, to 25.5 kcal/mol for **13**, and to 28.8 kcal/mol for **14** (B3PW91/6-31+G*//B3LYP/6-31G* + ZPE). The 5.1 kcal/mol difference in the E_a values for **14** and **12** is close to that of 4.5 kcal/mol for **4-syn** → **6-syn** and **9-syn** → **10-syn** (Figure 2). This suggests that its origin is the structural unit represented by **14**, rather than any steric contribution due to the third attached ring.

The relative insignificance of sterics is corroborated on inspection of the geometries of **4-syn** and **4-anti**, both of which exhibit comparable close contacts. Substituting the central hydrogen on a C−C=C unit by carbon (e.g., CH_3) decreases the angle size.[15] The CCC angles in the eight-membered ring at the cyclohexeno junctures in **4-syn** are 4−5° smaller than the corresponding angles in **9-syn** (Figure 3). A planar 1,3,5-cyclooctatriene would have internal CCC angles close to 135°, but puckering decreases this value. The eight-membered ring in **4-syn** is significantly less planar than that in **9-syn**, (Figure 3) and must undergo greater deformation than the latter to access its electrocyclization transition state (**TS6-syn**). This difference also causes the carbons involved in the Diels−Alder reaction to be closer to each other in **4-syn** relative to those in **9-syn** (Figure 3). Thus, the added cyclohexenofusion in **4-syn** simultaneously hinders electrocyclization and facilitates Diels−Alder reaction.

(15) For example, with B3LYP/6−31G*, the C=C−C angle in propene is 125.3°, compared to 122.1° in 2-methylpropene.

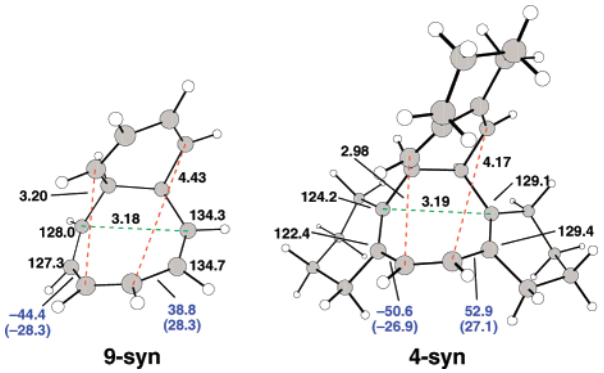

Figure 3. Selected distances (Å), CCC angles within the eight-membered ring (deg), and CCCC dihedral angles (deg, blue) from the B3LYP/6-31G* geometries of **9-syn** and **4-syn**. Values in parentheses pertain to the electrocyclization transition states. Red lines pertain to Diels−Alder reaction; green lines to electrocyclization.

In sum, our calculations on 1,5-di-*trans*-[12]annulene and its cyclohexenofused analog shed further light on the [12]annulene potential energy surface and provide an explanation for experimental results. The reaction course of the parent system can be altered by alkyl substituents. The alkyl groups cause greater puckering in the eight-membered ring resulting from the first electrocyclization of the di-trans-[12]annulene core. This translates into a higher barrier for benzene dimer formation and a lower barrier for intramolecular Diels−Alder reaction. The "tipping point" (i.e., the number of alkyl substituents at which the switchover occurs) remains to be determined. Finally, B3PW91 provides much more reliable relative energies than B3LYP for the parent system.

Acknowledgment. This work was supported by the NSF [CHE-0451241 (K.P.C.V.) and CHE-0553402 (C.C./W.L.K.)] and the ACS Petroleum Research Fund.

Supporting Information Available: Absolute energies and Cartesian coordinates for all stationary points; complete ref 14. This material is available free of charge via the Internet at http://pubs.acs.org.

OL8001915